JACS
JOURNAL OF THE AMERICAN CHEMICAL SOCIETY
Article
pubs.acs.org/JACS

Large-Scale Aqueous Synthesis of Fluorescent and Biocompatible Silicon Nanoparticles and Their Use as Highly Photostable Biological Probes

Yiling Zhong, Fei Peng, Feng Bao, Siyi Wang, Xiaoyuan Ji, Liu Yang, Yuanyuan Su, Shuit-Tong Lee,* and Yao He*

Institute of Functional Nano & Soft Materials (FUNSOM) and Jiangsu Key Laboratory for Carbon-Based Functional Materials & Devices, Soochow University, Suzhou 215123, China

Supporting Information

ABSTRACT: A large-scale synthetic strategy is developed for facile one-pot aqueous synthesis of silicon nanoparticles (SiNPs) yielding ~0.1 g SiNPs of small sizes (~2.2 nm) in 10 min. The as-prepared SiNPs feature strong fluorescence (photoluminescence quantum yield of 20−25%), favorable biocompatibility, and robust photo- and pH-stability. Moreover, the SiNPs are naturally water dispersible, requiring no additional post-treatment. Such SiNPs can serve as highly photostable bioprobes and are superbly suitable for long-term immunofluorescent cellular imaging.

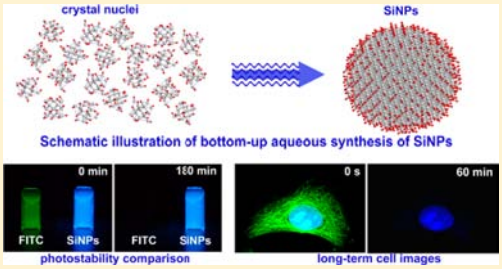

1. INTRODUCTION

There is a current interest in the development of silicon functional nanomaterials for a myriad of applications, owing to their many merits including excellent optical/electronic/mechanical properties, surface tailorability, compatibility with silicon technologies, etc.[1] Fluorescent silicon nanoparticles (SiNPs), as a representative zero-dimensional silicon nanomaterial, are highly promising for biological and biomedical applications, due to favorable biocompatibility and low toxicity.[2] However, SiNPs usually possess poor aqueous dispersibility due to surface-covered hydrophobic functional groups (e.g., Si−H bond). Recent years have seen much progress in producing hydrophilic SiNPs, including our photochemistry- and microwave-assisted synthesis of water-dispersible SiNPs.[3] Besides, methods have been reported to functionalize SiNPs with hydrophilic species (e.g., hydrophilic molecule, polymer, and micelle, etc),[4] to make the resultant SiNPs water dispersible and suitable for bioimaging applications. However, current synthetic methods usually require at least two independent steps to produce water-dispersible SiNPs. Typically, hydrophobic SiNPs are first prepared using large-size silicon nanomaterials as the silicon source (e.g., crystalline Si particles, SiO_x powders, bulk silicon, or silicon nanowires (SiNWs), etc); afterward, the hydrophobic SiNPs are modified with hydrophilic ligands to render them water dispersible (so-called "top-down" strategy). While those so-called top-down synthetic methods are workable, they involve relatively tedious procedures. Take our synthetic strategies as an example, hydrophobic SiNPs or SiNWs are required to be first prepared and then modified with hydrophilic ligands (e.g., acrylic acid, glutaric acid) to produce water-dispersible SiNPs.[3] However, the modification step invariably degrades the optical and surface properties of SiNPs (e.g., photoluminescent quantum yield (PLQY) of SiNPs decreases from 17% to <10% after micelle encapsulation).[4c] Consequently, effective methods for facile synthesis of water-dispersible fluorescent SiNPs are still much in demand.

Here we present a new aqueous synthetic approach, i.e., the "bottom-up"strategy, for facile one-pot synthesis of fluorescent SiNPs via *in situ* growth under microwave irradiation, by using hydrophilic molecules (e.g., 3-aminopropyl)trimethoxysilane, $C_6H_{17}NO_3Si$) as the silicon source. The as-prepared SiNPs have a small size of ~2.2 nm and are water dispersible, highly luminescent (PLQY: 20−25%), well biocompatible, strongly photo- and pH-stable, and superbly suitable for long-term cell imaging. In addition, our method is efficacious for large-scale and rapid synthesis of high-quality SiNPs, e.g., 0.1 g SiNPs are readily achieved in a 10 min reaction.

2. EXPERIMENTAL SECTION

2.1. Materials and Devices. (3-Aminopropyl)trimethoxysilane (97%) was purchased from Sigma-Aldrich. Trisodium citrate dihydrate (≥99.0%) was purchased from Sinopharm Chemical Reagent Co., Ltd. (China). CdSe/ZnS QDs were purchased from Wuhan Jiayuan Co., Ltd. (China). All chemicals were used without additional purification. All solutions were prepared using Milli-Q water (Millipore) as the solvent. The microwave system NOVA used for synthesizing SiNPs was made by Preekem of Shanghai, China. The system operates at 2450 MHz frequency and works at 0−500 W power. Exclusive vitreous vessels with a volume of 15 or 20 mL are equipped for the system to provide security during reaction demanding high temperature and pressure. The SiNPs were characterized by UV−vis absorption,

Received: March 13, 2013
Published: April 12, 2013

dx.doi.org/10.1021/ja4026227 | J. Am. Chem. Soc. 2013, 135, 8350−8356

photoluminescence (PL), transmission electronic microscopy (TEM), high-resolution TEM (HRTEM), Fourier-transform infrared (FTIR) spectroscopy, and laser-scanning confocal fluorescent microscopy. Optical measurements were performed at room temperature under ambient air conditions. UV−vis absorption spectra were recorded with a Perkin-Elmer lambda 750 UV−vis near-infrared spectrophotometer. PL measurements were performed using a HORIBA JOBTN YVON FLUOROMAX-4 spectrofluorimeter. The PLQY of samples was estimated using quinine sulfate in 0.1 M H_2SO_4 (literature quantum yield: 58%) as a reference standard, which was freshly prepared to reduce the measurement error.[5a] TEM and HRTEM samples were prepared by dispersing the sample onto carbon-coated copper grids with the excess solvent evaporated. The TEM/HRTEM overview images were recorded using Philips CM 200 electron microscope operated at 200 kV. For FTIR measurements, KBr was pressed into a slice, onto which the SiNPs sample was dropped. The solvent in the sample was adequately evaporated by irradiation (>30 min) with a high-power incandescent lamp. FTIR spectra were recorded on a Bruker HYPERION FTIR spectrometer and cumulated 32 scans at a resolution of 4 cm^{-1}. The powder X-ray diffraction (XRD) spectra were recorded on a Panalytical, Empyrean, X-ray diffractometer, operated at 40 mA and 40 kV. The SiNPs were placed on a zero-background sample holder made of monocrystal silicon plate. After evaporating the solvent, a film was formed and used for the measurement. Light-scattering analysis was performed using a DynaPro dynamic light scatterer (DLS), which was made by Malvern Corp, U.K. (ZEN3690). One mL SiNPs sample was transferred into an exclusive vitreous for DLS measurements. Experiment parameters were as follows: scan times: 100; dispersant: water; temperature: 25 °C; viscosity: 0.8872 cP; RI: 1.330; and dielectric constant: 78.5. Laser-scanning confocal fluorescent (Leica, TCS-SP5), equipped with diode laser (405 nm) and multiline argon laser (458, 476, 488, and 514 nm), was used for fluorescent cellular imaging. Images were captured and processed with image analysis software and were used for fluorescent cellular imaging. Images were captured and processed with image analysis software. Energy-dispersive X-ray (EDX) spectroscopy was utilized to determine the fraction of the resultant SiNPs. The SiNPs samples were first dispersed onto carbon-coated copper grids with the excess solvent evaporated and then characterized by using Philips CM 200 electron microscope, equipped with EDX spectroscopy.

2.2. Experimental Procedure. *2.2.1. Synthesis of SiNPs.* The SiNPs precursor solution was prepared by adding 100 mL of (3-aminopropyl)trimethoxysilane to 400 mL N_2-saturated aqueous solution dispersed with 18.6 g of trisodium citrate dihydrate. The mixture was stirred for 10 min. The resultant precursor solution was transferred into the exclusive vitreous vessel with a volume of 30 mL. The SiNPs with the maximum emission at ∼460 nm were prepared under 160 °C/15 min. After microwave irradiation, the SiNPs sample was removed when the temperature cooled to <30 °C naturally. It is worthwhile pointing out that, compared to the feeble luminescence of the precursor solution, the resultant SiNPs sample displayed intense blue-color fluorescence under UV irradiation (see Figure 2c).

To exclude impurities influence, such as (3-aminopropyl)-trimethoxysilane molecules and trisodium citrate dihydrate in solution, the residual reagents were removed by dialysis (1 kDa). The purified SiNPs aqueous solution with strong blue luminescence was investigated for photo- and pH-stability comparison, cytotoxicity assessment, and immunofluorescent cellular imaging.

Microwave dielectric heating is utilized in our method to take advantage of its three dominant merits compared to conventional convective heating. First, sample temperature can be rapidly raised due to the high utilization factor of microwave energy, leading to high reaction rate. Second, thermal gradient effects can be effectively reduced due to the volumetric heating of microwaves, which is favorable for homogeneous heating and uniform product formation. Finally, reaction selectivity is improved under microwave irradiation (MWI) due to different dipole constants of various substances.[5b−e] Moreover, the microwave method can be readily scaled up to large reaction volumes. Consequently, the MWI methodology has been widely applied for synthesizing various kinds of functional nanostructures (e.g., nanodots, nanorods, and nanowires).[6]

2.2.2. Photostability Comparison of FITC, CdTe and CdSe/ZnS QDs, and SiNPs. CdTe QDs were prepared based on our previous reports.[7] To guarantee reliable comparison, the PL intensity of FITC, CdTe and CdSe/ZnS QDs, and SiNPs was adjusted to the same value. The four samples were continuously irradiated for different time intervals using a 450 W xenon lamp of 365 nm.

2.2.3. MTT Assay of Cell Viability. Human epithelial cervical cancer cells (Hela) cells (in Dulbecco's modified eagle medium (DMEM) medium) were dispersed in 96-well plates (90 μL in each well containing 1×10^4 cells per well). Ten μL of the same SiNP solution as that used in the following cellular imaging was added to each well. Incubation was carried out for 0.5, 3, 12, and 48 h in a humidified atmosphere at 37 °C with 5% CO_2. The cytotoxicity of the SiNPs was evaluated by the MTT (3-(4,5-dimethylthiazol-2-yl)-2,5-diphenyltetrazolium bromide) assay (thiazolyl blue tetrazolium bromide (M5655)). The assay was based on the accumulation of dark-blue formazan crystals inside living cells after exposure to MTT, which is a well-established protocol for assessment of cellular viability.[8] Destruction of cell membranes by the addition of sodium dodecylsulfate resulted in the liberation and solubilization of crystals. The number of viable cells was thus directly proportional to the level of the initial formazan product created. The formazan concentration was finally quantified using a spectrophotometer by measuring the absorbance at 570 nm (ELISA reader). A linear relationship between cell number and optical density was established, thus allowing for accurate quantification of changes in the rate of cell proliferation.

2.2.4. pH Stability of SiNPs. The pH of the SiNPs aqueous solution was varied by dropwise addition of HCl or NaOH. The pH value was monitored by Seven Multi pH meter (Mettler Toledo), while concurrently the PL intensity of the samples was recorded by the HORIBA JOBTN YVON FLUOROMAX-4 spectrofluorimeter. In addition, the pH stability of SiNPs in DMEM medium containing 10% fetal bovine serum (FBS) at 37 °C was also measured.

2.2.5. Preparation of the SiNPs/Antibody Conjugates. The amino groups of SiNPs readily reacted with the carboxylic acid groups of the protein by using *N*-(3-dimethylaminopropyl)-*N*-ethylcarbodiimde hydrochloride (EDC) as zero length cross-linkers. Two μL EDC (6.4 mg/mL in H_2O) was first added to 12.5 μL goat antimouse IgG (4 mg/mL) in PBS buffer. The mixed solution was then incubated at 25 °C for 15 min to fully activate the carboxylic acid groups. Afterward, 110 μL SiNPs (in Milli-Q water, absorption value = 0.3, λ_{abs} = 345 nm) was added to the activated goat antimouse IgG. The resultant solution was incubated for 2 h at 25 °C under shaking in the dark and then kept overnight at 4 °C. No obvious precipitation was observed after this conjugation traction. The isourea byproduct and residual reagent (e.g., IgG with molecular weight of ∼168 KDa) were filtrated in the lower phase by using 300 KDa Nanosep centrifugal devices through centrifugation at 5000 rmp for 15 min. The upper phase containing the SiNPs/IgG conjugates was diluted by 30 μL PBS (pH = 7.4, 0.1 M) buffer. The final conjugates were stored at 4 °C in the dark for immunofluorescent cellular imaging.

2.2.6. Long-Term Immunofluorescent Labeling Hela Cells Using the SiNPs/Antibody Conjugates. Hela cells were cultured (37 °C, 5% CO_2) on a cover glass in DMEM with 10% heat-inactivated FBS and antibiotics (100 μg/mL streptomycin and 100 U/mL penicillin) overnight. For staining of nuclei, Hela cells were fixed with 4% sucrose and 4% paraformaldehyde for 20 min and blocked for 40 min in PBS containing 4% BSA and 0.1% Triton X-100. The fixed Hela cells were washed three times with PBS containing 0.1% Tween 20. To label nuclei, the fixed and blocked Hela cells were incubated sequentially with monoclonal anti-hn RNP for 1 h and goat antimouse IgG conjugated to SiNPs for 1 h. Then the stained cells were mounted on slides in fluoromount (Sigma, F4680) with coverslips. Samples were examined under a confocal laser microscope (Leica, TCS-SP5). Images were captured and processed with image analysis software. In using FITC as stain, all manipulations were identical to those mentioned above. Microtubules labeled by FITC were excited by argon laser ($\lambda_{excitation}$ = 488 nm) with 100 mW power, while the SiNPs-labeled

dx.doi.org/10.1021/ja4026227 | J. Am. Chem. Soc. 2013, 135, 8350−8356

nuclei were excited by diode laser ($\lambda_{excitation}$ = 405 nm) with 50 mW power. To guarantee fair comparison, argon and diode lasers at 15% and 30% power, respectively, were used in our experiment, so that the power values of these two laser sources were similar in such conditions for our equipment. Detection windows for SiNPs and FITC are 450−510 and 515−550 nm, respectively. Other conditions were the same in all comparison experiments. Images were captured with a cooled CCD camera at 15 s intervals for each color automatically.

3. RESULTS AND DISCUSSION

Our synthetic strategy is schematically illustrated in Scheme 1. In brief, $C_6H_{17}NO_3Si$ molecules are readily reduced by

Scheme 1. Schematic Illustration of Bottom-up One-Pot Synthesis of SiNPs[a]

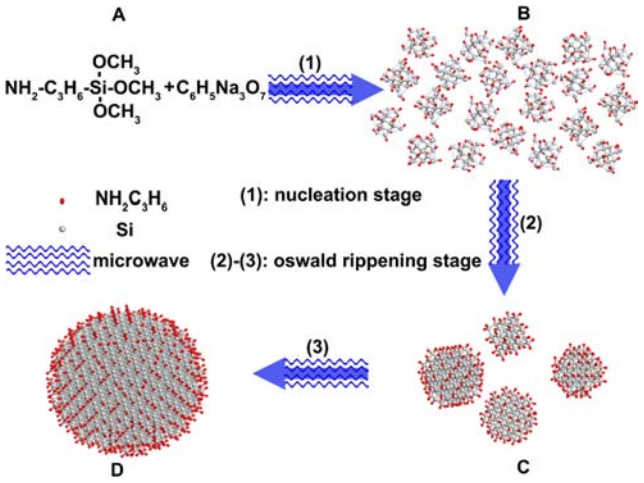

[a](A) reaction precursor; (B) 21 nuclei; and (C) 4 small-size and (D) 1 large-size nanocrystals. To simplify the model and ease comprehension, the effect of trisodium citrate dehydrate is ignored.

trisodium citrate ($C_6H_5Na_3O_7$ as reduction reagent) under microwave irradiation through an oxidation−reduction reaction, forming crystal nuclei in the first step (step 1: A → B). As the reaction proceeds, the concentration of $C_6H_{17}NO_3Si$ molecules decreases to a critical threshold and the nucleation stops. Afterward, the Ostwald ripening stage takes place and continues (steps 2 and 3). Typically, small-size nanocrystals are first formed in the initial Ostwald ripening stage (step 2: B → C). With further reaction, nanocrystal growth continues at the expense of dissolution and absorption of small nanocrystals of lower stability due to their larger surface-to-volume ratio, eventually producing more stable and larger-size silicon nanocrystals in the third step (step 3: C → D). Similar mechanism has been proposed for the growth of II−VI quantum dots in previous reports.[9]

Figure 1 displays the TEM and HRTEM images of SiNPs, in which the resultant SiNPs appear as spherical particles with good monodispersity. The well-resolved (220) lattice planes of ∼0.19 nm spacing in the HRTEM image (Figure 1b) demonstrate excellent crystallinity of the as-prepared SiNPs. Besides, a typical XRD pattern of the SiNPs showing the characteristic diffraction peaks of diamond structure Si, further confirms that the nanoscrystals are crystalline Si (Figure S1).[3e] The size distribution in Figure 1c, calculated by measuring more than 250 particles, shows an average diameter of 2.2 ± 0.7 nm. The diameter measured by dynamic light scattering (DLS) confirms the small size of the SiNPs with a hydrodynamic

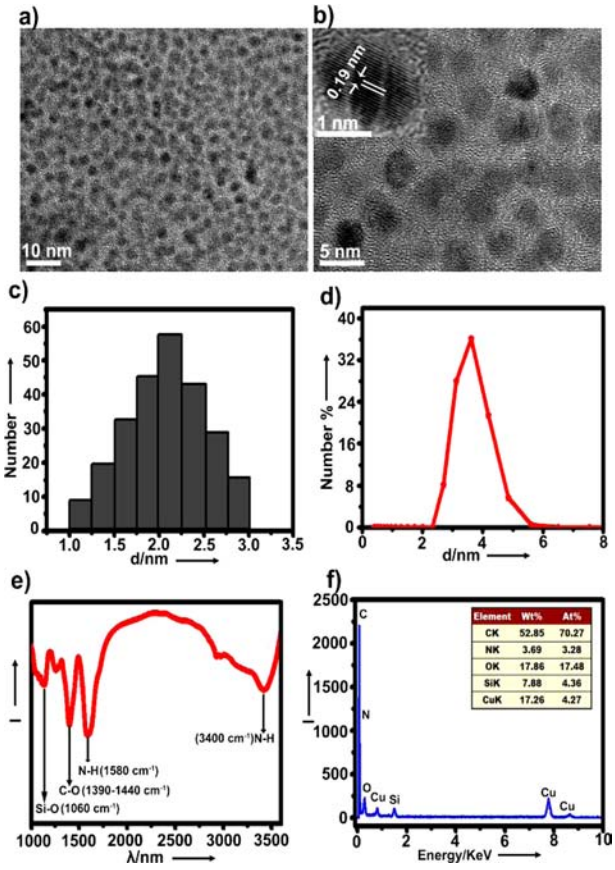

Figure 1. (a) TEM and (b) HRTEM images of the as-prepared SiNPs. Inset in (b) presents the enlarged HRTEM image of a single SiNP. (c) The TEM diameter distribution, (d) DLS, (e) FTIR spectra, and (f) EDX pattern of SiNPs. Table in the inset presents the elemental ratios (weight and atom percentages) calculated by the EDX software (K-shell intensity ratios are indicated).

diameter of ∼3.86 nm in Figure 1d. The small size offers great advantages for bioimaging, as particles with a diameter <10 nm feature quicker and easier renal clearance in vivo and less potential toxicity.[13] The different diameters measured by TEM and DLS are due to different surface states of the same sample under the two measurement conditions. Specifically, the solvent in the SiNPs sample must be strictly removed for TEM characterization, thus yielding a smaller diameter than that measured by DLS.[3c−e] To show the reaction-induced chemical bonding, FTIR spectra of the as-prepared SiNPs are measured (Figure 1e), which feature several distinct absorption peaks in the range of 1000−3500 cm^{-1}. Typically, the sharp absorbance peak at ∼1060 cm^{-1} is ascribed to the vibrational stretch of Si−O bonding. The strong absorbance at 1390−1440, 1580, and 3400 cm^{-1} are, respectively, assigned to the C−O and N−H bending vibrations and the N−H stretching vibration. The FTIR results demonstrate that the resultant SiNPs have a large amount of amino groups.[10] The EDX pattern reveals that the SiNPs contain Si, O, and N of 7.88, 17.86, and 3.69 % wt concentration, respectively (Figure 1f). The C and Cu weight concentrations listed in the table are not reliable since carbon-coated copper grids are used for the EDX measurement.

Figure 2a presents the normalized UV−PL spectra of the resultant SiNPs, indicating that the SiNPs possess good optical properties with clearly resolved absorption peaks and symmetrical PL peaks. In comparison to previously reported red-

dx.doi.org/10.1021/ja4026227 | J. Am. Chem. Soc. 2013, 135, 8350−8356

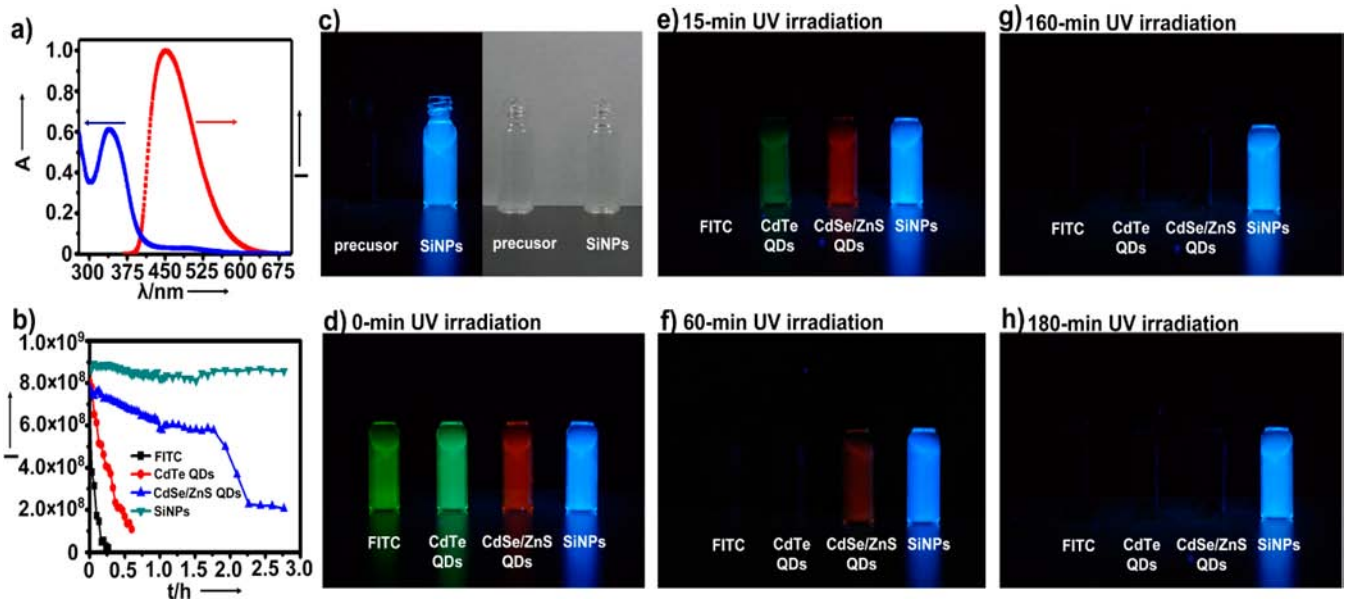

Figure 2. (a) Absorption and photoluminescence (UV−PL) spectra of the as-prepared SiNPs. (b) Photostability comparison of FITC, CdTe and CdSe/ZnS QDs, and SiNPs. (c) Photographs of SiNPs and reaction precursors solution under 365 nm irradiation (left) or ambient light (right). (d) Photographs of FITC, CdTe and CdSe/ZnS QDs, and SiNPs aqueous solution under UV irradiation for different time. All samples are continuously irradiated by a 450 W xenon lamp.

emitting (maximum emission wavelength (λ_{max} = 660 nm) SiNPs of ∼3.1 nm in diameter, the present SiNPs of much smaller sizes (∼2.2 nm) exhibit distinctly shorter λ_{max} (∼460 nm) due to quantum-size effect.[3d,e] Also, the strong fluorescence of the SiNPs (PLQY: 20−25%) is attributable to both quantum-size and ligand-related effects, similar to that in acrylic acid/allylamine-capped and polymer-coated SiNPs.[3a,b,4a,b] Significantly, as shown in Figure 2c, in comparison to the reaction precursor solution (i.e., $C_6H_{17}NO_3Si$ + $C_6H_5Na_3O_7$ solution), the aqueous solution of SiNPs shows distinct blue luminescence under UV irradiation, further demonstrating the strong fluorescence of the as-prepared SiNPs. The SiNPs feature excellent aqueous dispersibility due to surface-covered hydrophilic amino groups.[3,4] As a result, the SiNPs aqueous solution is highly transparent in the ambient environment. Furthermore, the SiNPs exhibit superior photostability compared to FITC dye and CdTe and CdSe/ZnS QDs (regarded as photostable fluorescent labels).[2] Figure 2b shows that the fluorescence of FITC is quickly quenched in 5 min UV irradiation due to severe photobleaching (black line), while the fluorescence of CdTe and CdSe/ZnS QDs, though comparatively more photostable, decreases to <50% in 2 h (red and blue lines) due to UV irradiation-induced surface deterioration.[9,11] In striking contrast, the fluorescence of SiNPs is extremely stable, preserving ∼90% of the initial intensity after 2 h of UV irradiation. Such remarkable photostability is attributed to the unique PL properties of SiNPs, similar to those in acrylic acid/allylamine-capped and polymer-coated SiNPs.[3,4] The photographs of the four samples of FITC, CdTe and CdSe/ZnS QDs, and SiNPs under UV irradiation are shown in Figure 2d−h. Notably, while all the samples exhibit distinct fluorescence during initial UV irradiation (Figure 2d), the fluorescent signals of the former three samples are gradually reduced with increasing irradiation time. Specifically, the fluorescence of FITC (Figure 2e), CdTe QDs (Figure 2f), and CdSe/ZnS QDs (Figure 2e) rapidly quenches in 15, 60, and 160 min UV irradiation, respectively. In remarkable contrast, the SiNPs sample preserves stable and bright fluorescence during long-time (e.g., 180 min) irradiation under the same experiment conditions (Figure 2h).

In order to use SiNPs in biological applications, we evaluate the cytotoxicity of the prepared SiNPs. Importantly, the SiNPs show insignificant cellular toxicity to cervical carcinoma Hela cells during 48 h incubation with the SiNPs (Figure 3a), with the same concentration as that used in the following cellular imaging experiments. Microscopic studies confirmed the biochemical assays of cellular viability. As shown in Figure 3b−f, no obvious morphological change of Hela cells was observed in the presence of SiNPs, when the incubation time is

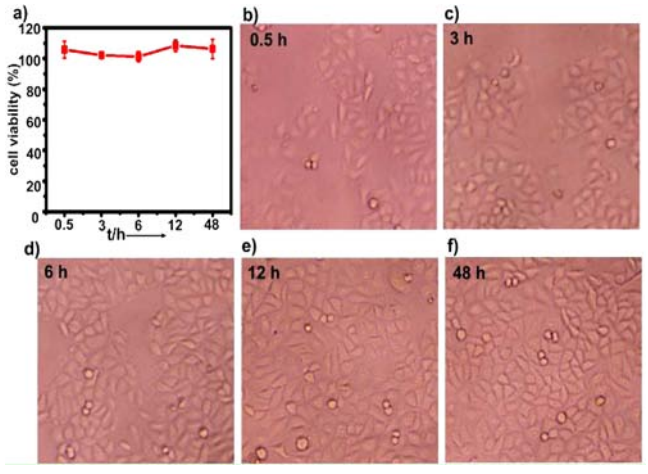

Figure 3. Cytotoxicity assessment of the as-prepared SiNPs. (a) Cell viability of Hela cells incubated with the SiNPs for different time. The cell viability was calculated as a percentage from the viability of the control (untreated) cells. The viability of the control cells was considered 100%. The results are means ± SD from three or four impendent experiments. (b−f) Morphology of Hela cells after incubated with SiNPs for 0.5, 3, 6, 12, and 48 h, respectively.

dx.doi.org/10.1021/ja4026227 | J. Am. Chem. Soc. 2013, 135, 8350−8356

extended to 48 h. These data suggest feeble cytotoxicity of the SiNPs to the cells, which is due to favorable biocompatibility of silicon and well consistent with previous reports.[2c,3]

As robust pH stability is essential to bioapplications,[2,3,4c,d] we thus further interrogate the pH stability of SiNPs. Notably, SiNPs in water maintain strong PL in the wide pH range of 4−11 (Figure 4a). Moreover, the pH stability of SiNPs in DMEM medium containing 10% FBS at 37 °C, the most relevant in vitro biological media, is also tested. Figure 4b shows that PL intensity only decreases slightly by ∼10% in acidic-to-basic environments in the pH range of 4−11. We attribute this robust pH stability to the plentiful surface-covered amino groups, which acts as a protective shell around the nanoparticle.[3a,d,e] The resultant SiNPs thus can be readily conjugated with protein (e.g., goat-antimouse IgG) via traditional EDC/NHS cross-linking reaction, i.e., the amino groups of ligands on SiNPs readily react with the carboxylic acid groups of the antibody via NHS and EDC as zero length cross-linkers (Figure 4c).[14] The as-prepared SiNPs/protein bioconjugates are highly transparent in ambient light and exhibit strong fluorescence under UV irradiation (Figure 4d). Remarkably, the bioconjugates possess excellent storage stability, maintaining bright and stable fluorescence after over 1 month storage in the ambient environment with no protection (Figure 4e).

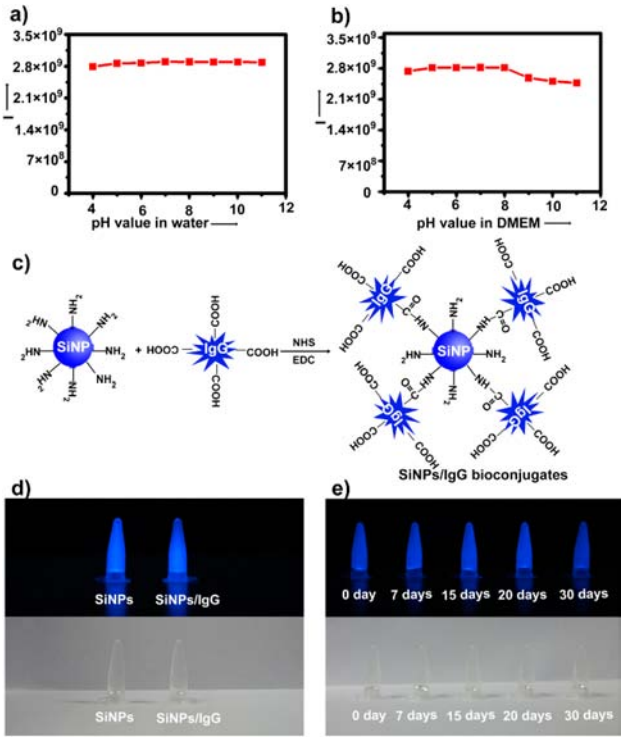

Figure 4. Temporal evolution of SiNPs fluorescence in (a) water and (b) DMEM solution under various pH values. (c) Schematic reaction of SiNPs with goat-antimouse IgG. The amino groups of SiNPs readily react with the carboxylic acid groups of IgG via EDC/NHS cross-linking reaction (figure not to scale). (d) Optical micrographs of the SiNPs/IgG bioconjugates under UV (365 nm) irradiation. (e) The SiNPs/IgG bioconjugates display stable and bright fluorescence under UV irradiation and maintain high transparency during 30 day storage in ambient environment without any protection.

The resultant biofunctional and fluorescent SiNPs/protein bioconjugates are further explored as biological fluorescent probes for immunofluorescent cell labeling. Based on highly specific antibody−antigen immunoreactions, the resultant SiNPs bioconjugates are specifically targeted to the nuclei of Hela cells, which are preincubated with a nuclei-specific anti-hn RNP antibody.[3a,d,e] Figure 5a shows the fluorescence of the SiNPs-labeled nuclei (blue) and the FITC-labeled cellular microtubules (green) is intense and clearly spectrally resolved, respectively. Significantly, the SiNPs are particularly suitable for long-term cellular imaging due to their high photostability. In our experiment, the SiNP-labeled nuclei yield stable fluorescent signals during a 60 min continuous observation (Figure 5b), in good accord with the excellent photostability of SiNPs as discussed above. In contrast, the signals from FITC fluorescent labels almost completely disappear in short-time irradiation, and the green fluorescence of FITC rapidly diminishes in 3 min due to severe photobleaching (Figure 5b).

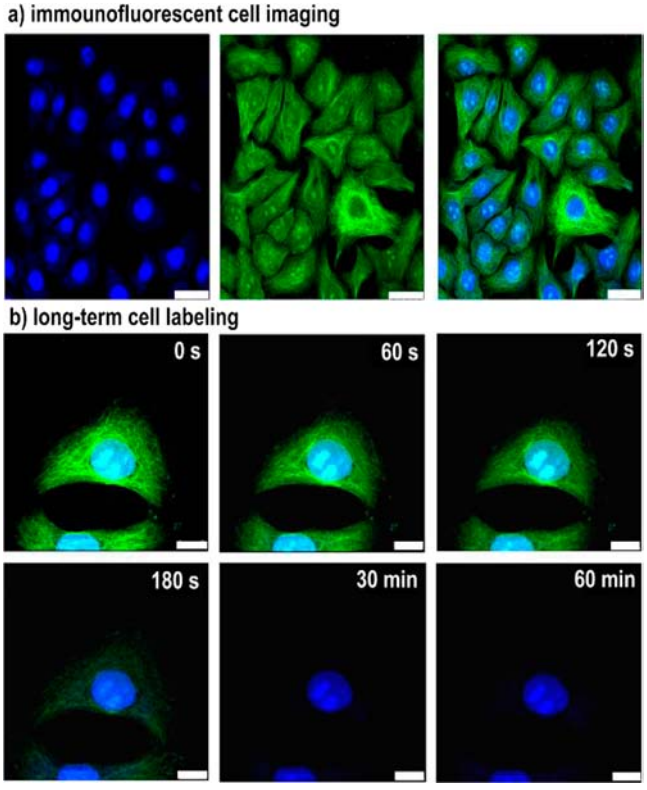

Figure 5. Photos of immunofluorescent cell images captured by laser scanning confocal microscopy. (a) Left: nuclei are distinctively labeled by SiNPs (excitation: 405 nm, detection window: 450−510 nm); middle: microtubules are distinctively labeled by FITC (excitation: 488 nm, detection window: 515−550 nm); and right: superposition of the two fluorescence images. (b) Time-dependent stability comparison of fluorescence signals of Hela cells labeled by SiNPs (blue) and FITC (green). Scale bar = 5 μm.

4. CONCLUSION

In summary, we have developed a one-pot bottom-up strategy for the facile, rapid, and large-scale synthesis of SiNPs in water. Significantly, the as-prepared SiNPs feature excellent aqueous dispersibility, ultrahigh photo- and pH-stability, strong PL, and favorable biocompatibility. Cellular experiments show the SiNPs are superbly suitable for long-term and real-time cellular imaging. The present synthetic strategy makes use of simple kitchen chemistry and does not require expensive equipment

dx.doi.org/10.1021/ja4026227 | J. Am. Chem. Soc. 2013, 135, 8350−8356

and harsh conditions, in contrast to the previous synthetic methods involving tedious and complicated manipulation. Furthermore, a large quantity of SiNPs can be rapidly prepared, e.g., 0.1 g SiNPs is readily produced in 10 min reaction. Consequently, the present large-scale aqueous synthesis of high-quality SiNPs will facilitate a myriad of applications of SiNPs, such as in solar cells, biosensors, in vitro and in vivo imaging, etc.[1,2]

■ ASSOCIATED CONTENT

Supporting Information

Figure S1 and corresponding discussion. This information is available free of charge via the Internet at http://pubs.acs.org.

■ AUTHOR INFORMATION

Corresponding Author

apannale@suda.edu.cn; yaohe@suda.edu.cn

Notes

The authors declare no competing financial interest.

■ ACKNOWLEDGMENTS

This work was supported by National Basic Research Program of China (973 Program 2013CB934400, 2012CB932400), NSFC (30900338, 51072126), and a Project Funded by the Priority Academic Program Development of Jiangsu Higher Education Institutions (PAPD).

■ REFERENCES

(1) (a) Pavesi, L.; Negro, L. D.; Mazzoleni, C.; Franzo, G.; Priolo, F. *Nature* **2000**, *408*, 440−444. (b) Ding, Z. F.; Quinn, B. M.; Haram, S. K.; Pell, L. E.; Korgel, B. A.; Bard, A. J. *Science* **2002**, *296*, 1293−1297. (c) Ma, D. D. D.; Lee, C. S.; Au, F. C. K.; Tong, S. Y.; Lee, S. T. *Science* **2003**, *299*, 1874−1877. (d) Patolsky, F.; Timko, B. P.; Yu, G. H.; Fang, Y.; Greytak, A. B.; Zheng, G. F.; Lieber, C. M. *Science* **2006**, *313*, 1100−1104. (e) Allen, J. E.; Hemesath, E. R.; Perea, D. E.; Lensch- Falk, J. L.; Li, Z. Y.; Yin, F.; Gass, M. H.; Wang, P.; Bleloch, A. L.; Palmer, R. E.; Lauhon, L. *J. Nat. Nanotechnol.* **2008**, *3*, 168−173. (f) Shao, M. W.; Cheng, L.; Zhang, X. H.; Ma, D. D. D.; Lee, S. T. *J. Am. Chem. Soc.* **2009**, *131*, 17738−17739. (g) He, Y.; Su, S.; Xu, T. T.; Zhong, Y. L.; Zapien, J. A.; Li, J.; Fan, C. H.; Lee, S. T. *Nano Today* **2011**, *6*, 122−130. (h) Su, S.; Wei, X. P.; Zhong, Y. L.; Guo, Y. Y.; Su, Y. Y.; Huang, Q.; Lee, S. T.; Fan, C. H.; He, Y. *ACS Nano* **2012**, *6*, 2582−2590. (i) Su, Y. Y.; Wei, X. P.; Peng, F.; Zhong, Y. L.; Lu, Y. M.; Su, S.; Xu, T. T.; Lee, S. T.; He, Y. *Nano Lett.* **2012**, *12*, 1845−1850.

(2) (a) Michalet, X.; Pinaud, F. F.; Bentolila, L. A.; Tsay, J. M.; Doose, S.; Li, J. J.; Sundaresan, G.; Wu, A. M.; Gambhir, S. S.; Weiss, S. *Science* **2005**, *307*, 538−544. (b) Song, S. P.; Qin, Y.; He, Y.; Huang, Q.; Fan, C. H.; Chen, H. Y. *Chem. Soc. Rev.* **2010**, *39*, 4234−4243. (c) He, Y.; Fan, C. H.; Lee, S. T. *Nano Today* **2010**, *5*, 282−295.

(3) (a) He, Y.; Su, Y. Y.; Yang, X. B.; Kang, Z. H.; Xu, T. T.; Zhang, R. Q.; Fan, C. H.; Lee, S. T. *J. Am. Chem. Soc.* **2009**, *131*, 4434−4438. (b) He, Y.; Kang, Z. H.; Li, Q. S.; Tsang, C. H. A.; Fan, C. H.; Lee, S. T. *Angew. Chem., Int. Ed.* **2009**, *48*, 128−132. (c) He, Y.; Zhong, Y. L.; Peng, F.; Wei, X. P.; Su, Y. Y.; Su, S.; Gu, W.; Liao, L. S.; Lee, S. T. *Angew. Chem., Int. Ed.* **2011**, *50*, 3080−3083. (d) He, Y.; Zhong, Y. Y.; Peng, F.; Wei, X. P.; Su, Y. Y.; Lu, Y. M.; Su, S.; Gu, W.; Liao, L. S.; Lee, S. T. *J. Am. Chem. Soc.* **2011**, *133*, 14192−14195. (e) Zhong, Y. L.; Peng, F.; Wei, X. P.; Zhou, Y. F.; Wang, J.; Jiang, X. X.; Su, Y. Y.; Su, S.; Lee, S. T.; He, Y. *Angew. Chem., Int. Ed.* **2012**, *51*, 8485−8489.

(4) (a) Li, Z. F.; Ruckenstein, E. *Nano Lett.* **2004**, *4*, 1463−1467. (b) Warner, J. H.; Hoshino, A.; Yamamoto, K.; Tilley, R. D. *Angew. Chem., Int. Ed.* **2005**, *44*, 4550−4554. (c) Erogbogbo, F.; Yong, K. T.; Roy, I.; Xu, G. X.; Prasad, P. N.; Swihart, M. T. *ACS Nano* **2008**, *2*, 873−878. (d) Erogbogbo, F.; Yong, K. T.; Roy, I.; Hu, R.; Law, W. C.; Zhao, W. W.; Ding, H.; Wu, F.; Kumar, R.; Swihart, M.; Prasad, P. N. *ACS Nano* **2011**, *5*, 413−423. (e) Shiohara, A.; Hanada, S.; Prabakar, S.; Fujioka, K.; Lim, T. H.; Yamamoto, K.; Northcote, P.; Tilley, R. D. *J. Am. Chem. Soc.* **2010**, *132*, 248−253. (f) Atkins, T. M.; Thibert, A.; Larsen, D. S.; Dey, S.; Browning, N. D.; Kauzlarich, S. M. *J. Am. Chem. Soc.* **2011**, *133*, 20664−20667. (g) Sato, K.; Yokosuka, S.; Takigami, Y.; Hirakuri, K.; Fujioka, K.; Manome, Y.; Sukegawa, H.; Iwai, H.; Fukata, N. *J. Am. Chem. Soc.* **2011**, *133*, 18626−18633. (h) Mastronardi, M. L.; Maier-Flaig, F.; Faulkner, D.; Henderson, E. J.; Kübel, C.; Lemmer, U.; Ozin, G. A. *Nano Lett.* **2012**, *12*, 337−342. (i) Guan, M.; Wang, W. D.; Henderson, E. J.; Dag, o; Kübel, C.; Chakravadhanula, V. S. K.; Rinck, J.; Moudrakovski, I. L.; Thomson, J.; McDowell, J.; Powell, A. K.; Zhang, H. X.; Ozin, G. A. *J. Am. Chem. Soc.* **2012**, *134*, 8439−8446.

(5) (a) Wang, X. H.; Qu, K. G.; Xu, B. L.; Ren, J. S.; Qu, X. G. *J. Mater. Chem.* **2011**, *21*, 2445−2450. (b) Michael, D.; Mingo, P.; Baghurst, D. R. *Chem. Soc. Rev.* **1991**, *20*, 1−47. (c) Galema, S. A. *Chem. Soc. Rev.* **1997**, *26*, 233−238. (d) Muccioli, G. G.; Wouters, J.; Poupaert, J. H.; Norberg, B.; Poppitz, W.; Scriba, G. K. E.; Lambert, D. M. *Org. Lett.* **2003**, *5*, 3599−3602. (e) Ju, Y. H.; Varma, R. S. *Tetrahedron Lett.* **2005**, *46*, 6011−6014.

(6) (a) Gerbec, J. A.; Magana, D.; Washington, A.; Strouse, G. F. *J. Am. Chem. Soc.* **2005**, *127*, 15791−15800. (b) Panda, A. B.; Glaspell, G.; El-Shall, M. S. *J. Am. Chem. Soc.* **2006**, *128*, 2790−2791. (c) Washington ll, A. L.; Strouse, G. F. *J. Am. Chem. Soc.* **2008**, *130*, 8961−8922. (d) Kim, S. H.; Lee, S. Y.; Yi, G. R.; Pine, D. J.; Yang, S. M. *J. Am. Chem. Soc.* **2006**, *128*, 10897−10904. (e) He, Y.; Kang, Z. H.; Li, Q. S.; Tsang, C. H. A.; Fan, C. H.; Lee, S. T. *Angew. Chem., Int. Ed.* **2009**, *48*, 128−132. (f) He, Y.; Su, Y. Y.; Yang, X. B.; Kang, Z. H.; Xu, T. T.; Zhang, R. Q.; Fan, C. H.; Lee, S. T. *J. Am. Chem. Soc.* **2009**, *131*, 4434−4438. (g) He, Y.; Zhong, Y. L.; Su, Y. Y.; Lu, Y. M.; Jiang, Z. Y.; Peng, F.; Xu, T. T.; Su, S.; Huang, Q.; Fan, C. H.; Lee, S. T. *Angew. Chem., Int. Ed.* **2011**, *123*, 5813−5816.

(7) (a) He, Y.; Lu, H. T.; Sai, L. M.; Lai, W. Y.; Fan, Q. L.; Wang, L. H.; Huang, W. *J. Phys. Chem. B* **2006**, *110*, 13370−13374. (b) He, Y.; Lu, H. T.; Sai, L. M.; Lai, W. Y.; Fan, Q. L.; Wang, L. H.; Huang, W. *J. Phys. Chem. B* **2006**, *110*, 13352−13356. (c) He, Y.; Sai, L. M.; Lu, H. T.; Hu, M.; Lai, W. Y.; Fan, Q. L.; Wang, L. H.; Huang, W. *Chem. Mater.* **2007**, *19*, 359−365. (d) He, Y.; Lu, H. T.; Sai, L. M.; Su, Y. Y.; Hu, M.; Fan, C. H.; Wang, L. H.; Huang, W. *Adv. Mater.* **2008**, *20*, 3416−3421.

(8) (a) Su, Y. Y.; He, Y.; Lu, H. T.; Sai, L. M.; Li, Q. N.; Li, W. X.; Wang, L. H.; Shen, P. P.; Huang, Q.; Fan, C. H. *Biomaterials* **2009**, *30*, 19−25. (b) Su, Y. Y.; Peng, F.; Jiang, Z. Y.; Zhong, Y. L.; Lu, Y. M.; Jiang, X. X.; Huang, Q.; Fan, C. H.; Lee, S. T.; He, Y. *Biomaterials* **2011**, *32*, 5855−5862.

(9) (a) He, Y.; Lu, H. T.; Sai, L. M.; Lai, W. Y.; Fan, Q. L.; Wang, L. H.; Huang, W. *J. Phys. Chem. B* **2006**, *110*, 13370−13374. (b) He, Y.; Lu, H. T.; Sai, L. M.; Lai, W. Y.; Fan, Q. L.; Wang, L. H.; Huang, W. *J. Phys. Chem. B* **2006**, *110*, 13352−13356. (c) He, Y.; Sai, L. M.; Lu, H. T.; Hu, M.; Lai, W. Y.; Fan, Q. L.; Wang, L. H.; Huang, W. *Chem. Mater.* **2007**, *19*, 359−365. (d) He, Y.; Lu, H. T.; Sai, L. M.; Su, Y. Y.; Hu, M.; Fan, C. H.; Huang, W.; Wang, L. H. *Adv. Mater.* **2008**, *20*, 3416−3421.

(10) (a) Kato, Y.; Yamazaki, H.; Tomozawa, M. *J. Am. Chem. Soc.* **2001**, *84*, 2111−2116. (b) Bansal, V.; Ahmad, A.; Sastry, M. *J. Am. Chem. Soc.* **2006**, *128*, 14059−14066. (c) He, J. L.; Ba, Y.; Ratcliffe, C. I.; Ripmeester, J. A.; Klug, D. D.; Tse, J. S.; Preston, K. F. *J. Am. Chem. Soc.* **1998**, *120*, 10697−10705. (d) He, Y.; Zhong, Y. Y.; Peng, F.; Wei, X. P.; Su, Y. Y.; Lu, Y. M.; Su, S.; Gu, W.; Liao, L. S.; Lee, S. T. *J. Am. Chem. Soc.* **2011**, *133*, 14192−14195. (e) Dancil, K. P. S.; Greiner, D. P.; Sailor, M. J. *J. Am. Chem. Soc.* **1999**, *121*, 7925−7930. (f) Frey, B. L.; Corn, R. M. *Anal. Chem.* **1996**, *68*, 3187−3193.

(11) Gaponik, N.; Talapin, D. V.; Rogach, A. L.; Hoppe, K.; Shevchenko, E. V.; Kornowski, A.; Eychmuller, A.; Weller, H. *J. Phys. Chem. B* **2002**, *116*, 7177−7185.

(12) (a) Li, Z. F.; Ruckenstein, E. *Nano Lett.* **2004**, *4*, 1463−1467. (b) Warner, J. H.; Hoshino, A.; Yamamoto, K.; Tilley, R. D. *Angew. Chem., Int. Ed.* **2005**, *44*, 4550−4554. (c) Erogbogbo, F.; Yong, K. T.; Roy, I.; Xu, G. X.; Prasad, P. N.; Swihart, M. T. *ACS Nano* **2008**, *2*, 873−878. (d) He, Y.; Fan, C. H.; Lee, S. T. *Nano Today* **2010**, *5*, 282−

295. (e) Erogbogbo, F.; Yong, K. T.; Roy, I.; Hu, R.; Law, W. C.; Zhao, W. W.; Ding, H.; Wu, F.; Kumar, R.; Swihart, M.; Prasad, P. N. *ACS Nano* **2011**, *5*, 413−423.
(13) (a) Choi, H. S.; Liu, W.; Misra, P.; Tanaka, E.; Zimmer, J. P.; Ipe, B. I.; Bawendi, M. G.; Frangioni, J. V. *Nat. Biotechnol.* **2007**, *25*, 1165−1170. (b) Su, Y. Y.; Peng, F.; Jiang, Z. Y.; Zhong, Y. L.; Lu, Y. M.; Jiang, X. X.; Huang, Q.; Fan, C. H.; Lee, S. T.; He, Y. *Biomaterials* **2011**, *32*, 5855−5862. (c) He, Y.; Zhong, Y. L.; Su, Y. Y.; Lu, Y. M.; Jiang, Z. Y.; Peng, F.; Xu, T. T.; Su, S.; Huang, Q.; Fan, C. H.; Lee, S. T. *Angew. Chem., Int. Ed.* **2011**, *123*, 5813−5816.
(14) (a) Wang, S. P.; Mamedova, N.; Kotov, N. A.; Chen, W.; Studer, J. *Nano Lett.* **2002**, *2*, 817−822. (b) Xing, Y.; Chaudry, Q.; Shen, C.; Kong, K. Y.; Zhau, H. E.; Chung, L. W.; Petros, J. A.; O'Regan, R. M.; Yezhelyev, M. V.; Simons, J. W.; Wang, M. D.; Nie, S. M. *Nat. Protoc.* **2007**, *2*, 1152−1165.